NANOMOLAR PULSE DIPOLAR EPR SPECTROSCOPY IN PROTEINS USING COMMERCIAL LABELS AND HARDWARE

Katrin Ackermann, Joshua L. Wort, Bela E. Bode*

EaStCHEM School of Chemistry, Biomedical Sciences Research Complex and Centre of Magnetic Resonance, University of St Andrews, St Andrews, KY16 9ST, Scotland

Abstract: The study of complex biomolecular assemblies implicated in human health and disease is increasingly performed under native conditions. Pulse Dipolar Electron paramagnetic resonance (PDEPR) spectroscopy is a powerful tool that provides highly precise geometric constraints in frozen solution, however the drive towards *in cellulo* EPR is limited by the currently achievable concentration sensitivity in the low µM regime. Achieving PDEPR at physiologically relevant sub-µM concentrations is currently very challenging. Recently, relaxation induced dipolar modulation enhancement (RIDME) measurements using a combination of nitroxide and double-histidine Cu^{II} based spin labels allowed measuring 500 nM concentration of a model protein. Herein, we demonstrate Cu^{II}-Cu^{II} RIDME and nitroxide-nitroxide PELDOR measurements down to 500 and 100 nM protein concentration, respectively. This is possible using commercial instrumentation and spin labels. These results herald a transition towards routine sub-µM PDEPR measurements at short to intermediate distances (~1.5-3.5 nm), without the necessity of specialized instrumentation or spin-labelling protocols, particularly relevant for applications in near physiological conditions.

The study of increasingly complex biomolecular assemblies and their interactions with the cellular environment has driven interest towards holistic structural characterization under conditions with high biological validity. Pulse dipolar EPR (PDEPR) is a powerful tool for such characterization, and complements X-ray crystallography, NMR, Förster resonance energy transfer (FRET), and cryo-EM data by providing solution-state distance constraints in systems of virtually unlimited size and complexity.[1] Due to these characteristics, PDEPR is also an emerging technique for conformational studies of protein and nucleic acid complexes *in cellulo*.[2] However, physiological concentrations are often in the sub-µM regime. In combination with low numbers of cells within samples, the challenge is to achieve sufficient absolute sensitivity. Analyzing a representative sample of 61 recent applications of nitroxide-nitroxide pulsed electron-electron double resonance (PELDOR)[3] measurements using the 4-pulse double electron-electron resonance (DEER)[4] sequence reveals the use of spin concentrations between 5 and 400 µM (median 100 µM, mean 116 ± 90 µM, see SI) demonstrating the current state of the art. Recently, Cu^{II}-nitroxide 5-pulse relaxation induced dipolar modulation enhancement (RIDME)[5] measurements at 500 nM concentration in a protein *in vitro* allowed not only precise distance measurements but also determination of the binding affinity.[6] Thereby, demonstrating the high-affinity of genetically encoded double-histidine motifs to Cu^{II} ions,[7] and their suitability as labelling sites for low concentration studies. Herein, we approach practical concentration limits associated with PDEPR experiments and found Cu^{II}-Cu^{II} RIDME measurements and nitroxide-nitroxide PELDOR measurements feasible at 500 nM and 100 nM protein concentration, respectively (corresponding to spin concentration of 1.6 µM and 200 nM, respectively). Importantly, these measurements were performed in a commercial non-broadband Q-band spectrometer, using commercial spin labels, methanethiosulfonate (MTSL)[8] and Cu^{II}-nitrilotriacetic acid (Cu^{II}-NTA)[7b] (figure 1). To our knowledge this is the first demonstration of sub-µM Cu^{II}-Cu^{II} and NO-NO PDEPR measurements in a biological system.

Commercial instruments have been used successfully for PELDOR measurements at low µM concentration.[9] Enhanced concentration sensitivity can be further improved *via* homebuilt high-power resonator-free spectrometers[10] or by implementation of arbitrary waveform generators (AWGs) and shaped pulses that yield higher spin inversion efficiencies.[11] Additionally, novel pulse sequences have shown to enhance measurement sensitivity.[12] Trityl-based radicals[13] with exquisitely narrow spectral linewidths, have been measured at 180 nM spin concentration[13c] employing the single-frequency double quantum coherence (DQC)[14] experiment. Nevertheless, this concentration regime has not been demonstrated for the most used DEER experiment on nitroxide labels.

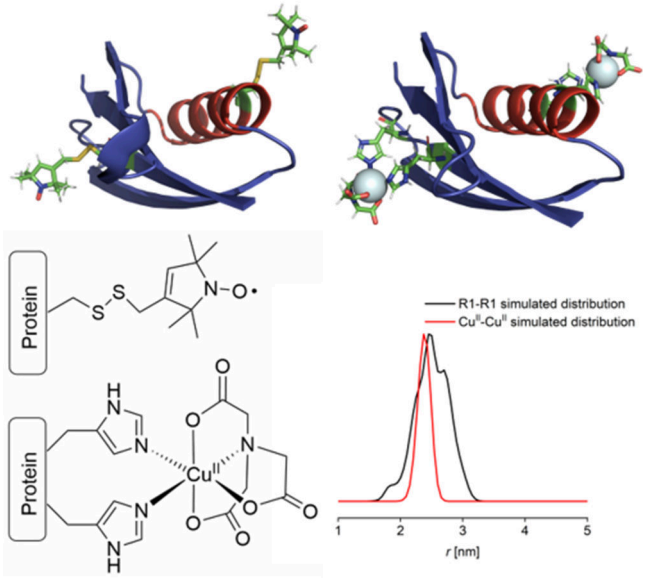

Figure 1. GB1 constructs, spin label structures and simulated distance distributions. Top: Cartoon representations of GB1 constructs I6R1/K28R1 (left) and I6H/N8H/K28H/Q32H (right), with spin labels shown in stick representation. Bottom: Chemical structures of R1 nitroxide and double histidine Cu^{II}-NTA spin labels (left). Corresponding simulated distance distribution (right) for each construct, shown in black and red, respectively.

In the current study, *Streptococcus sp.* Group G protein G, B1 domain (GB1) constructs (I6R1/K28R1 and I6H/N8H/K28H/Q32H) were used as biological model systems (figure 1). GB1 has been used extensively in previous EPR methodology studies.[6,7,15] We have shown previously that nitroxide-detected Cu^{II}-nitroxide and Cu^{II}-Cu^{II} RIDME are similar in sensitivity and roughly two orders of magnitude more sensitive than Cu^{II}-Cu^{II} PELDOR when limited to rectangular pulses.[6] Here, we endeavored to test the sensitivity of the most widespread pulse dipolar EPR methodology, nitroxide-nitroxide PELDOR. Therefore Cu^{II}-Cu^{II} RIDME and nitroxide-nitroxide PELDOR were measured at 500 nM concentration, for a direct comparison of experiment sensitivity (figure 2). The optimum temperatures with respect to sensitivity were found to be 30 K and 50 K, respectively (see SI). As RIDME is a single frequency technique, it can be performed with all pulses coinciding with the resonance frequency of the resonator and thus benefits in sensitivity compared to double frequency techniques, such as the 4-pulse DEER sequence where detection is generally performed off resonance. This sensitivity gain in dependence of the cavity quality factor being adjusted to meet the required bandwidth could be quantified as approximately a factor 2 (see SI). Furthermore, the influence of instantaneous diffusion (that occurs when dephasing is induced by dipolarly coupled spins being inverted by detection pulses reducing the detected echo) was shown to be negligible in the I6R1/K28R1 construct at both 500 nM and 25 µM concentrations (see SI).

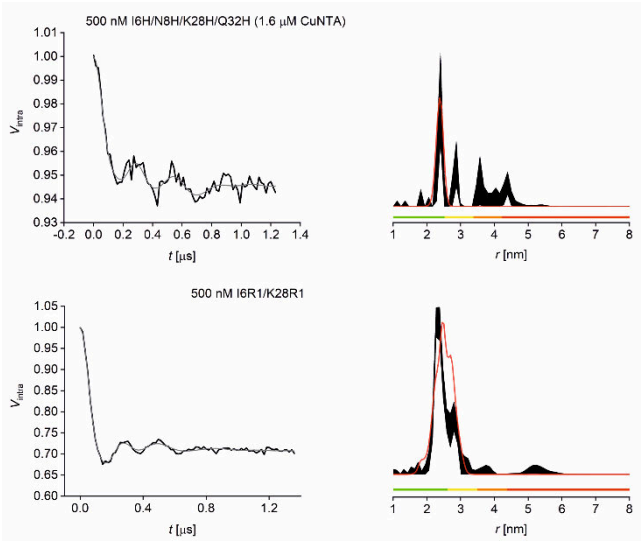

Figure 2. 500 nM GB1 Cu^{II}-Cu^{II} RIDME and NO-NO PELDOR Q-band data at 30 and 50K, respectively. Top: RIDME data for 500 nM GB1 tetra-histidine with 1.6 µM Cu^{II}-NTA added. Bottom: PELDOR data for 500 nM GB1 I6R1/K28R1. Left: Background-corrected data (black) and fit (grey). Right: Corresponding distance distributions given as 95% confidence intervals (± 2σ) with 50% noise added for error estimation during statistical analysis; simulated distance distributions are shown in red. Color bars represent reliability ranges (green: shape reliable; yellow: mean and width reliable; orange: mean reliable; red: no quantification possible).

For the Cu^{II}-Cu^{II} RIDME data shown in figure 2, only the distance peak at ~2.5 nm was shown to be stable upon data validation. Additional measurements at 500 µM protein concentration suggested the distribution peaks > 2.5 nm were artefacts, insignificant in the 95% confidence interval (see SI). This indicated that measurements at 500 nM tetra-histidine protein concentration likely approached the lower concentration limit for Cu^{II}-Cu^{II} RIDME in our hands. It should be noted that the poor modulation depth (5.5%) is a result of the limiting affinity of Cu^{II}-NTA for the β-sheet double histidine motif.[6] Pulse dipolar EPR methods allow precise determination of binding affinities from PELDOR[16] and RIDME[17] data. The observed modulation depth is consistent with predictions using binding affinities previously derived from Cu^{II}-nitroxide RIDME pseudo-titration[6] and extrapolated ITC data (see SI). Conversely, for the nitroxide-nitroxide PELDOR data the bimodal distribution shown in figure 2 was recapitulated in additional measurements at 25 µM I6R1/K28R1 protein concentration (see SI). This suggested that measurements at 500 nM protein concentration were not yet testing the lower concentration limit for nitroxide-nitroxide PELDOR. To test this hypothesis, nitroxide-nitroxide PELDOR was also measured at 100 nM protein concentration (figure 3).

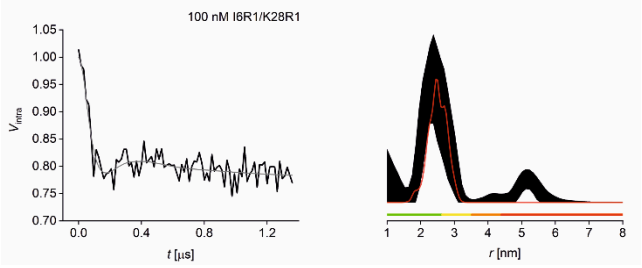

Figure 3. 100 nM GB1 Q-band PELDOR data at 50K. Left: Background-corrected PELDOR data (black) and fit (grey) for 100 nM I6R1/K28R1 GB1. Right: Corresponding distance distribution given as 95% confidence intervals (± 2σ) with 50% noise added for error estimation during statistical analysis; simulated distance distributions are shown in red. Color bars represent reliability ranges (green: shape reliable; yellow: mean and width reliable; orange: mean reliable; red: no quantification possible).

The nitroxide-nitroxide PELDOR data shown in figure 3 indicate that at 100 nM the retrieved experimental distribution is no longer bimodal, however the mean distance is still retrieved as the only significant peak following data validation. Nevertheless, the relatively poor signal-to-noise ratio mandates a regularization parameter that does not allow resolving both distance populations (SI). This suggests that 100 nM approaches the minimum concentration achievable for reliable distance distributions from nitroxide-nitroxide PELDOR under our conditions. Sensitivity analysis suggests that measurement of I6R1/K28R1 at 100 nM is a factor ~15 worse than measurement at 500 nM, rather than just a factor 5 as would be expected from the concentration difference alone. The additional factor 3 may be considered as a penalty for imperfect measurement optimization at very low concentrations (see SI). Further comparison of relative sensitivities for nitroxide-nitroxide PELDOR against Cu^{II}-Cu^{II} RIDME revealed approximately a factor 10 difference (see SI).

This gain in sensitivity for nitroxide-nitroxide PELDOR compared to Cu^{II}-Cu^{II} RIDME can be summarized by considering 3 contributing factors: i) gain of a factor 5 in the modulation depth (29% vs 5.5%, respectively), ii) further gain of a factor ~7 in increased signal (i.e., echo amplitude), and iii) loss of a factor ~3.5 by a twelvefold slower averaging rate. This analysis clearly indicates that modulation depth is a limiting factor for Cu^{II}-Cu^{II} RIDME sensitivity. This is to be expected for a non-covalent spin-labelling strategy with dissociation constants in the high nM, and low µM regime. It should be noted that a tetra-histidine construct containing a pair of α-helical double histidine motifs may be expected to achieve modulation depths > 12% for Cu^{II}-Cu^{II} RIDME under similar labelling conditions (see SI). Possible strategies to further improve modulation depths include insertion of an artificial amino-acid bearing a covalent Cu^{II} centre to overcome the limiting equilibrium constants,[18] or measuring nitroxide detected Cu^{II}-nitroxide RIDME in excess of Cu^{II} chelate spin label, to shift the binding equilibrium far to the right and achieve modulation depths approaching 50%, regardless of protein concentration.

Taken together, results from this and our previous study[6] suggest that Cu^{II}-nitroxide RIDME may be an additional factor ~1.5 more sensitive than nitroxide-nitroxide PELDOR, and thus could allow measurements even below 100 nM protein concentration benchmarked herein (see SI).

In conclusion, these findings showcase that in favorable circumstances superb concentration sensitivities are achievable using commercial instrumentation and spin labels. In the case of the widely applied nitroxide-nitroxide 4-pulse PELDOR experiment, concentration sensitivities orders of magnitude greater than routine (≥10 µM) are possible using rectangular pulses at Q-band frequencies. Nevertheless, long distances will be a challenge at these low concentrations. Additionally, Cu^{II}-Cu^{II} RIDME measurements showcase that systems unamenable to conventional thiol-based covalent spin labelling are also accessible in the sub-µM concentration regime, when used in conjunction with double-histidine motifs. Indeed, benchmarking this new sensitivity threshold is truly promising as a pathway to novel science, and may facilitate study of systems previously thought to be beyond the scope of pulse EPR spectroscopy. Perhaps most importantly, our results emphasize that commercial instrumentation possesses sufficient concentration sensitivity to facilitate a transition towards routine measurements in the sub-µM concentration regime.

Acknowledgement

We gratefully acknowledge Prof. Sunil Saxena for the kind gift of the original GB1 plasmid used in this study. This study was supported by previous equipment grants through the Wellcome Trust (099149/Z/12/Z) and BBSRC (BB/R013780/1). We gratefully acknowledge ISSF support to the University of St Andrews from The Wellcome Trust. BEB and KA acknowledge support by the Leverhulme Trust (RPG-2018–397). JLW is supported by the BBSRC DTP Eastbio.

References

(1) (a) Verhalen, B.; Dastvan, R.; Thangapandian, S.; Peskova, Y.; Kotieche, H. A.; Nakamoto, R. K.; Tajkhorshid, E.; Mchaourab, H. S. *Nature* **2017**, *543*, 738-741. (b) Duss, O.; Michel, E.; Yulikov, M.; Schubert, M.; Jeschke, G.; Allain, F. H. T. *Nature* **2014**, *509*, 588-592. (c) Kapsalis, C.; Wang, B.; El Mkami, H.; Pitt, S. J.; Lippiat, J. D.; Bode, B. E.; Pliotas, C. *Nat. Commun.,* **2019**, *10*, 4619. (d) Schmidt, T.; Wälti, M. A.; Baber, J. L.; Hustedt, E. J.; Clore, M. G. *Angew. Chem. Int. Ed.* **2016**, *55*, 15905-15909. (e) Sameach, H.; Ghosh, S.; Gervokyan-Airapetov, L.; Saxena, S.; Ruthstein, S. *Angew. Chem. Int. Ed.* **2019**, *58*, 3053-3056. (f) Joseph, B.; Sikora, A.; Bordignon, E.; Jeschke, G.; Cafiso, D. S.; Prisner, T. F. *Angew. Chem. Int. Ed.* **2015**, *54*, 6196-6199. (g) Ghosh, S.; Lawless, M. J.; Brubaker, H. J.; Singewald, K.; Kurpiewski, M. R.; Jen-Jacobsen, L.; Saxena, S. *Nucleic Acids Res.* **2020**, *48*, e49.

(2) (a) Theillet, F.; Binolfi, A.; Bekei, B.; Martorana, A.; Honor, M. R.; Stuiver, M.; Verzini, S.; Lorenz, D.; van Rossum, M.; Goldfarb, D.; Selenko, P. *Nature* **2016**, *530*, 45-50. (b) Igarashi, R.; Sakai, T.; Hara, H.; Tenno, T.; Tanaka, T.; Tochio, H.; Shirakawa, M. *J. Am. Chem. Soc.* **2010**, *132*, 8228-8229. (c) Azarkh, M.; Beiber, A.; Qi, M.; Fischer, J. W. A.; Yulikov, M.; Godt, A.; Drescher, M. *J. Phys. Chem. Lett.* **2019**, *10*, 1477-1481. (d) Krstić, I. B.; Hänsel-Hertsch, R.; Romainczyk, O.; Engels, J. W.; Dötsch, V.; Prisner, T. F. *Angew. Chem. Int. Ed.* **2011**, *50*, 5070-5074. (e) Yang, Y.; Chen, S.; Yang, F.; Li, X.; Feintuch, A.; Su, X.; Goldfarb, D. *Proc. NatI. Acad. Sci. U.S.A* **2020**, *117*, 20566-20575. (f) Joseph, B.; Sikora, A.; Cafiso, D. S. *J. Am. Chem. Soc.* **2016**, *138*, 1844.

(3) (a) Milov, A. D.; Salikhov, K. M.; Schirov, M. D. *Fiz. Tverd. Tela.* **1981**, *23*, 975. (b) Milov, A. D.; Ponomarev, A. B.; Tsvetkov, Y. D. *Chem. Phys. Lett.,* **1984**, *110*, 67-72.

(4) Pannier, M.; Viet, S.; Godt, A.; Jeschke, G.; Spiess, H. W. *J. Magn. Reson.* **2000**, *142*, 331-340.

(5) Milikisyants, S.; Scarpelli, F.; Finiguerra, M. G.; Ubbink, M.; Huber, M. *J. Magn. Reson.* **2009**, *201*, 48-56.

(6) Wort, J. L.; Ackermann, K.; Giannoulis, A.; Stewart, A. J.; Norman, D. G.; Bode, B. E. *Angew. Chem. Int. Ed.* **2019**, *58*, 11861-11865.

(7) (a) Cunningham, T. F.; Putterman, M. R.; Desai, A.; Horne, W. S.; Saxena, S. *Angew. Chem. Int. Ed.* **2015**, *54*, 6330-6334. (b) Ghosh, S; Lawless, M. J.; Rule, G. S.; Saxena, S. *J. Magn. Reson.* **2018**, *286*, 163-171.

(8) (a) Berliner, L. J.; Grunwald, J.; Hankovszky, H. O.; Hideg, K. *Anal. Biochem.* **1982**, *119*, 450–455. (b) Hubbell, W. L.; Altenbach, C. *Curr. Opin. Struct. Biol.* **1994**, *4*, 566-573.

(9) Babaylova, E. S.; Malygin, A. A.; Lomzov, A. A.; Pyshnyi, D. V.; Yulikov, M.; Jeschke, G.; Krumkacheva, O. A.; Fedin, M. V.; Karpova, G. G.; Bagryanskaya, E. G. *Nuc. Acids. Res.* **2016**, *44*, 7935-7943.

(10) (a) Cruickshank, P. A. S.; Bolton, D. R.; Robertson, D. A.; Hunter, R. I.; Wylde, R. J.; Smith, G. M. *Rev. Sci. Instrum.* **2009**, *80*, 103102. (b) Hofbauer, W.; Earle, K. A.; Dunnam, C. R.; Moscicki, J. K.; Freed, J. H. *Rev. Sci. Instrum.* **2004**, *75*, 1194.

(11) (a) Motion, C. L.; Cassidy, S. L.; Cruickshank, P. A.; Hunter, R. I.; Bolton, D. R.; El Mkami, H.; Van Doorslaer, S.; Lovett, J. E.; Smith, G. M. *J. Magn. Reson.* **2017**, *278*, 122-133. (b) Spindler,

P. E.; Zhang, Y.; Endeward, B.; Gershernzon, N.; Skinner, T. E.; Glasser, S. J.; Prisner, T. F. *J. Magn. Reson.* **2012**, *218*, 49-58. (c) Doll, A.; Pribitzer, S.; Tschaggelar R.; Jeschke, G. *J. Magn. Reson.* **2013**, *230*, 27-39. (d) Spindler, P. E.; Glaser, S. J.; Skinner, T. E.; Prisner, T. F. *Angew. Chem. Int. Ed.* **2013**, *52*, 3425-3429. (e) Breitgoff, F. D.; Keller, K.; Qi, M.; Klose, D.; Yulikov, M.; Godt, A.; Jeschke, G. *J. Magn. Reson.* **2019**, *308*, 106560.
(12) (a) Borbat, P. P.; Georgieva, E. R.; Freed, J. H. *J. Phys. Chem. Lett.* **2013**, *4*, 170-175. (b) Spindler, P. E.; Waclawska, I.; Endeward, B.; Plackmeyer, J.; Ziegler, C.; Prisner, T. F. *J. Phys. Chem. Lett.* **2015**, *6*, 4331-4335. (c) Bahrenberg, T.; Yang, Y.; Goldfarb, D.; Feintuch, A. *Magnetochemistry* **2019**, *5*, 20. (d) Doll, A.; Qi, M.; Pribitzer, S.; Wili, N.; Yulikov, M.; Godt, A.; Jeschke, G. *Phys. Chem. Chem. Phys.* **2015**, 17, 7334-7344.
(13) (a) Reginsson, G. W.; Kunjir, N. C.; Sigurdsson, S. T.; Schiemann, O. *Chem. Eur. J.* **2012**, *18*, 13580-13584. (b) Yang, Z.; Lui, Y.; Borbat, P.; Zweier, J. L.; Freed, J. H.; Hubbell, W. L. *J. Am. Chem. Soc.* **2012**, *134*, 9950-9952. (c) Fleck, N.; Heubach, C. A.; Hett, T.; Haege, F. R.; Bawol, P. P.; Baltruschat, H.; Schiemann, O. *Angew. Chem. Int. Ed.* **2020**, *59*, 2-8.
(14) Borbat, P. P; Freed, J. H. *Chem. Phys. Lett.* **1999**, *313*, 145-154.
(15) (a) Giannoulis, A.; Yang, Y.; Gon, Y.; Tan, X.; Feintuch, A.; Carmieli, R.; Bahrenberg, T.; Liu Y.; Su, X.; Goldfarb, D. *Phys. Chem. Chem. Phys.* **2019**, *21*, 10217-10227. (b) Jarvi, A. G.; Cunningham, T. F.; Saxena, S. *Phys. Chem. Chem. Phys.* **2019**, *21*, 10238-10243. (c) Jarvi, A. G.; Ranguelova, K.; Ghosh, S.; Weber, R. T.; Saxena, S. *J. Phys. Chem. B* **2018**, *122*, 10669-10677.
(16) (a) Bode, B. E.; Margraf, D.; Plackmeyer, J.; Dürner, G.; Prisner, T. F.; Schiemann, O. *J. Am. Chem. Soc.* **2007**, *129*, 6736-6745. (b) Ackermann, K.; Giannoulis, A.; Cordes, D. B.; Slawin, A. M. Z; Bode, B. E. *Chem. Commun.* **2015**, *51*, 5257-5260. (c) Giannoulis, A.; Ackermann, K.; Spindler, P. E.; Higgins, C.; Cordes, D. B.; Slawin, A. M. Z.; Prisner, T. F.; Bode, B. E. *Phys. Chem. Chem. Phys.* **2018**, *20*, 11196-11205.
(17) Giannoulis, A.; Oranges, M.; Bode, B. E. *ChemPhysChem.,* **2017**, *18, 2318-2321.*
(18) Merz, G.; Borbat, P. P.; Muok, A. R.; Srivastava, M.; Bunck, D. N.; Freed, J. H.; Crane, B. R. *J. Phys. Chem. B* **2018**, *122*, 9443-9451.